AGU ADVANCING EARTH AND SPACE SCIENCES

Geophysical Research Letters

RESEARCH LETTER
10.1029/2023GL102853

Karst Groundwater Vulnerability Determined by Modeled Age and Residence Time Tracers

MaryLynn Musgrove[1], Bryant C. Jurgens[2], and Stephen P. Opsahl[3]

[1]U.S. Geological Survey, Oklahoma-Texas Water Science Center, Austin, TX, USA, [2]U.S. Geological Survey, California Water Science Center, Sacramento, CA, USA, [3]U.S. Geological Survey, Oklahoma-Texas Water Science Center, San Antonio, TX, USA

Key Points:

- Groundwater age tracers provide unique insight into the vulnerability of karst groundwater to land-surface contamination
- The complicated hydrologic structure of karst nonetheless follows similar patterns as other aquifers
- Independent geochemical tracers of residence time provide proxies for vulnerability determined from age tracers

Supporting Information:

Supporting Information may be found in the online version of this article.

Correspondence to:

M. Musgrove,
mmusgrov@usgs.gov

Citation:

Musgrove, M., Jurgens, B. C., & Opsahl, S. P. (2023). Karst groundwater vulnerability determined by modeled age and residence time tracers. *Geophysical Research Letters*, *50*, e2023GL102853. https://doi.org/10.1029/2023GL102853

Received 27 JAN 2023
Accepted 18 AUG 2023

Author Contributions:

Conceptualization: MaryLynn Musgrove, Bryant C. Jurgens, Stephen P. Opsahl
Investigation: MaryLynn Musgrove, Stephen P. Opsahl
Methodology: Bryant C. Jurgens
Software: Bryant C. Jurgens
Visualization: MaryLynn Musgrove
Writing – original draft: MaryLynn Musgrove
Writing – review & editing: MaryLynn Musgrove, Bryant C. Jurgens, Stephen P. Opsahl

Abstract Karst aquifers are a vital groundwater resource globally, but features such as rapid recharge and conduit flow make them highly vulnerable to land-surface contamination. We apply environmental age tracers to the south-central Texas Edwards aquifer, a karst resource in a rapidly urbanizing and drought-prone region, to assess vulnerability to land-surface contamination and risks unique to karst aquifers. We show that vulnerability of Edwards aquifer groundwater follows similar spatial and depth patterns common to porous-media type aquifers, despite complicated karst hydrogeologic features. Shallow and unconfined parts are more vulnerable to land-surface contamination than the deeper and confined parts, although even the oldest groundwater is mixed with some recent recharge. When modeled age-tracer results are coupled with other independent geochemical tracers of water-rock interaction specific to karst settings, they can yield insight into residence time and associated vulnerability.

Plain Language Summary Understanding groundwater contamination risks is crucial for resource management. Karst aquifers—formed by the dissolution of soluble rocks such as limestone—supply as much as a quarter of the world's drinking water. Karst aquifers are highly complex and vulnerable to contamination by human activities. Groundwater age provides direct insight into the vulnerability of groundwater to contamination. Here we use groundwater ages (ranging from 4 to 16,900 years) and other geochemical tracers for the Edwards aquifer, a critical karst resource in Texas in a rapidly urbanizing and climatically sensitive area, to assess vulnerability to contamination, with implications for karst aquifers globally. This approach provides new insights not independently possible from hydrogeologic characteristics or age tracers.

1. Introduction

Understanding the vulnerability of water resources to contamination—anthropogenic or geogenic—is requisite for resource assessment and management. Groundwater age or residence time—that is, the time since groundwater recharge occurred—provides a foundation for understanding an aquifer's vulnerability to contamination (Jasechko et al., 2017) and sustainability for human and ecosystem needs (Ferguson et al., 2020). Karst aquifers develop in soluble rocks such as carbonates, occur in >140 countries, cover about 15% of the ice-free continental surface, and supply water for 10%–25% of the global population (Ford & Williams, 2007; Stevanović, 2019). Unique karst characteristics—for example, focused recharge, conduit flow, heterogeneity, strong surface water/groundwater interaction, and high yields—allow little time for contaminant filtration or sorption. Karst aquifers are recognized for their vulnerability to surface-loaded contamination (Hartmann et al., 2021), but their dynamic and complex hydrogeology makes characterization of vulnerability difficult (Ford & Williams, 2007; Hess & White, 1988; White, 1988). In addition to hydrologic sensitivity, karst regions are often defined by ecologic sensitivity (e.g., Humphreys, 2011), both of which might be enhanced in drought-prone or urban growth areas. The Edwards aquifer in south-central Texas, United States (U.S.), exemplifies these features—a critical, hydrologically-complex, karst resource in a rapidly urbanizing, drought-prone region. The aquifer is also a uniquely diverse but endangered ecosystem (Bowles & Arsuffi, 1993).

Groundwater age cannot be directly measured, rather environmental age tracers associated with recharge are used with analytical models of idealized tracer transport to interpret the age distribution of a sample. Commonly referred to as lumped parameter models (LPMs), the models provide a distribution of ages that can vary in shape, resembling a Gaussian or exponential distribution, and can be unimodal or bimodal. When calibrated to tracer data, the LPMs estimate a sample's mixture of ages and mean age. As tools for estimating groundwater age distributions have become more sophisticated and available, they have demonstrated unique value for understanding aquifers and quantitatively assessing vulnerability (e.g., Solder et al., 2020). We apply tracer-derived age metrics to assess vulnerability in a complex karst aquifer. Groundwater samples from 81 wells, analyzed for a large range of geochemical constituents (including age interpretations for 60 samples), allow for a comprehensive aquifer assessment. We compare age interpretations with anthropogenic contamination effects, aquifer and well characteristics, and independent geochemical tracers of residence time. Results indicate that although the Edwards aquifer exhibits complex spatial and temporal variability consistent with the complexities of karst, systematic patterns of age and vulnerability are regionally evident. This context is valuable for assessing other complex karst aquifers.

2. Karst and the Edwards Aquifer

The karstic Edwards aquifer is highly productive and an important regional resource (Sharp & Banner, 1997); it is a designated sole-source aquifer that serves >2 million people (Smith et al., 2005; U.S. Environmental Protection Agency, 2022). Groundwater divides separate the aquifer into segments. We focus on the largest, which includes San Antonio—the second most populous Texas city; like many karst regions, the area is rapidly urbanizing (U.S. Census Bureau, 2022), accompanied by potential increases in anthropogenic contaminants (e.g., Mahler & Massei, 2007; Musgrove et al., 2016).

The aquifer extends in a narrow southwest-northeast band (Figure 1), along which aquifer rocks dip steeply to the south/southeast. Miocene-age faulting offsets aquifer rocks, forming the confined and unconfined zones (Maclay & Small, 1983); aquifer units are progressively deeper downdip. The aquifer is highly transmissive with flow focused in permeable units; regional flow is complex and controlled by faulting (Lindgren et al., 2004; Maclay & Small, 1983). Downdip the aquifer rapidly transitions to saline groundwater (Schultz, 1994). Watersheds of upland streams that flow to the south and east define the contributing zone. Streamflow losses across the recharge zone provide most recharge, with natural discharge at large springs (Lindgren et al., 2004). Annual rainfall is highly variable and the region is drought prone (Griffiths & Strauss, 1985).

3. Methods

3.1. Sampling and Analysis

Groundwater samples were collected from 81 sites during 2017–2018 and analyzed for a range of organic and inorganic constituents, including environmental age tracers. Sampling, analysis, and quality-control are described in Kingsbury et al. (2021) and Musgrove et al. (2023). Data are provided in a companion data release (Musgrove et al., 2023).

Samples, grouped by well networks, were collected once from 32 public-supply wells (PSWs), 19 domestic supply wells (including three production wells), and 30 observation (monitoring) wells (MWs). Most PSWs were in the aquifer's downdip confined zone, whereas most domestic wells were in the unconfined recharge zone. MWs were in the unconfined zone in urbanized northern San Antonio.

Analysis included nonparametric statistics and land-use characterization. Statistical results with $p < 0.05$ were considered significant (only $p < 0.05$ results are reported). Land use was characterized by 500-m buffers for sites (2012 data; Falcone, 2015), assigning a dominant (>50%) category (natural, urban, agricultural, or mixed).

3.2. Environmental Age Tracers

A suite of age tracers (tritium [^{3}H], carbon-14 [^{14}C], sulfur hexafluoride [SF_6], dissolved and noble gases, and tritiogenic helium-3 [$^3He_{trit}$]) were analyzed for most PSWs and domestic wells and a subset ($n = 10$) of MWs (^{3}H was collected at all wells). Age distributions for each sample were determined by fitting tracer concentrations to an LPM using the TracerLPM computer program (Jurgens et al., 2012). See Figure S1 in Supporting Information S1, for common groundwater age distributions. Inverse modeling was guided by preliminary classification based on ^{3}H concentrations (Lindsey et al., 2019): *Modern* groundwater is almost wholly recharged after 1953; *PreModern* groundwater is almost wholly recharged before 1953 and may be thousands of years old; *Mixed* groundwater contains substantial portions of both *Modern* and *PreModern* water. Model concentrations of

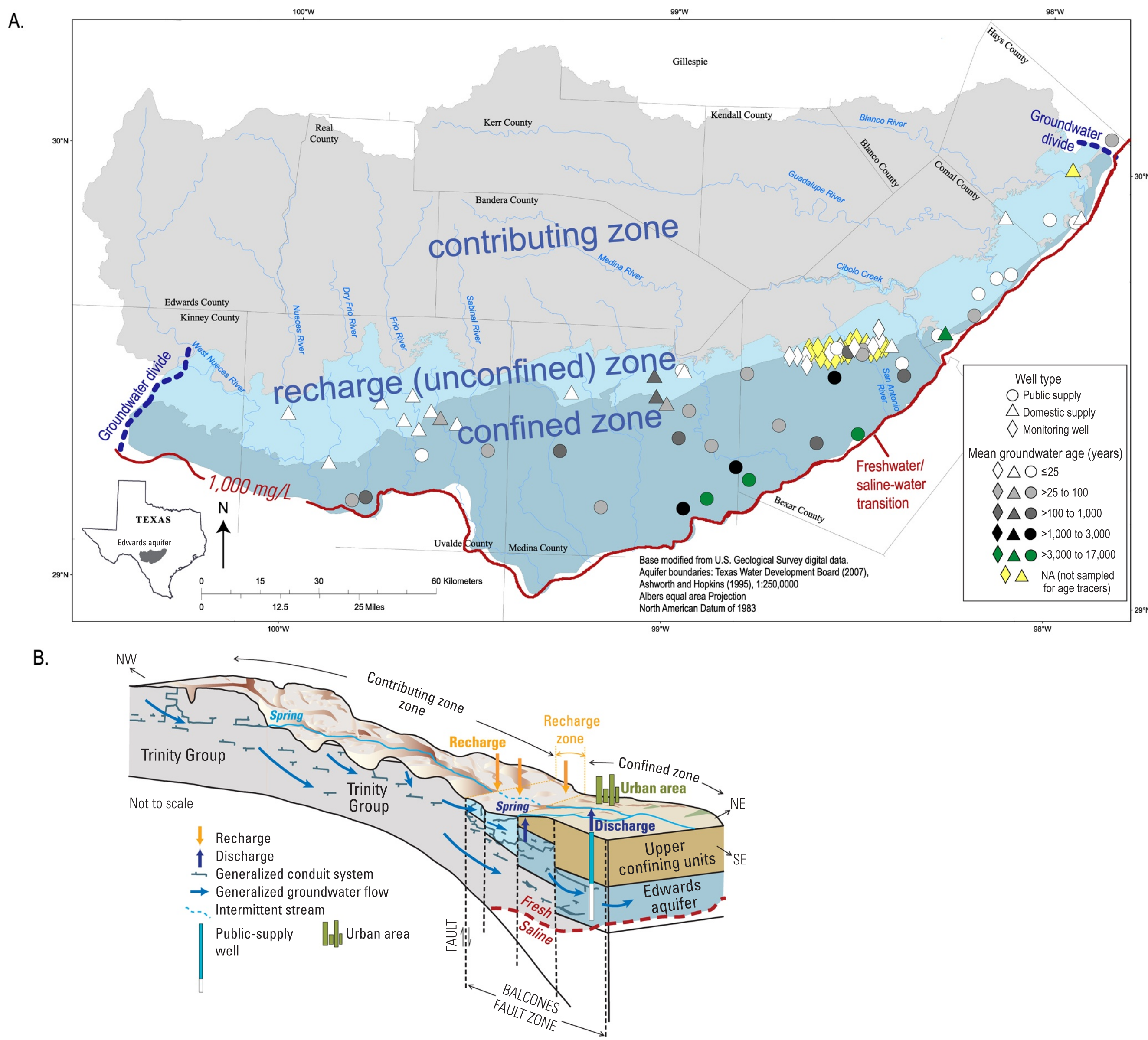

Figure 1. The Edwards aquifer's San Antonio segment: (a) sample locations by well type and mean groundwater ages (Ashworth & Hopkins, 1995; Texas Water Development Board, 2007). (b). Schematic north-northwest to south-southeast aquifer cross section and conceptual model. Modified from Musgrove et al. (2014).

tracers, which can account for effects of dispersion and mixing, are computed by convolution of the LPMs with observed atmospheric tracer histories (Jurgens et al., 2012). A sample's age distribution is computed by varying the mean age and (or) fraction of *Modern* water until the difference between modeled and measured concentrations for all tracers is minimized. Inverse modeling was aided by graphs of tracer concentrations in relation to LPM output to identify potential models and age ranges. As input to LPMs, gas tracers (SF_6, $^3He_{trit}$, and $^4He_{rad}$) were corrected for contributions resulting from solubility equilibrium, excess air, gas fractionation, and terrigenic helium by using the DGMETA program (Jurgens et al., 2020). ^{14}C concentrations were corrected for dilution by carbonate minerals by scaling the atmospheric ^{14}C input to match the ^{14}C content of *Modern* groundwater. Each tracer has associated uncertainties; thus, inclusion of multiple tracers often improves age models. Not all tracers were interpreted for all samples because of analytical limitations or suitability of results. Final LPM selections were based on model fit and conceptual reasonability and are detailed in Musgrove et al. (2023). A dispersion model (DM) or 2-component mixture (binary-mixing-model [BMM]) of *Modern* water and an older component where each is described by a DM (BMM-DM-DM) (Jurgens et al., 2012) consistently provided the most realistic

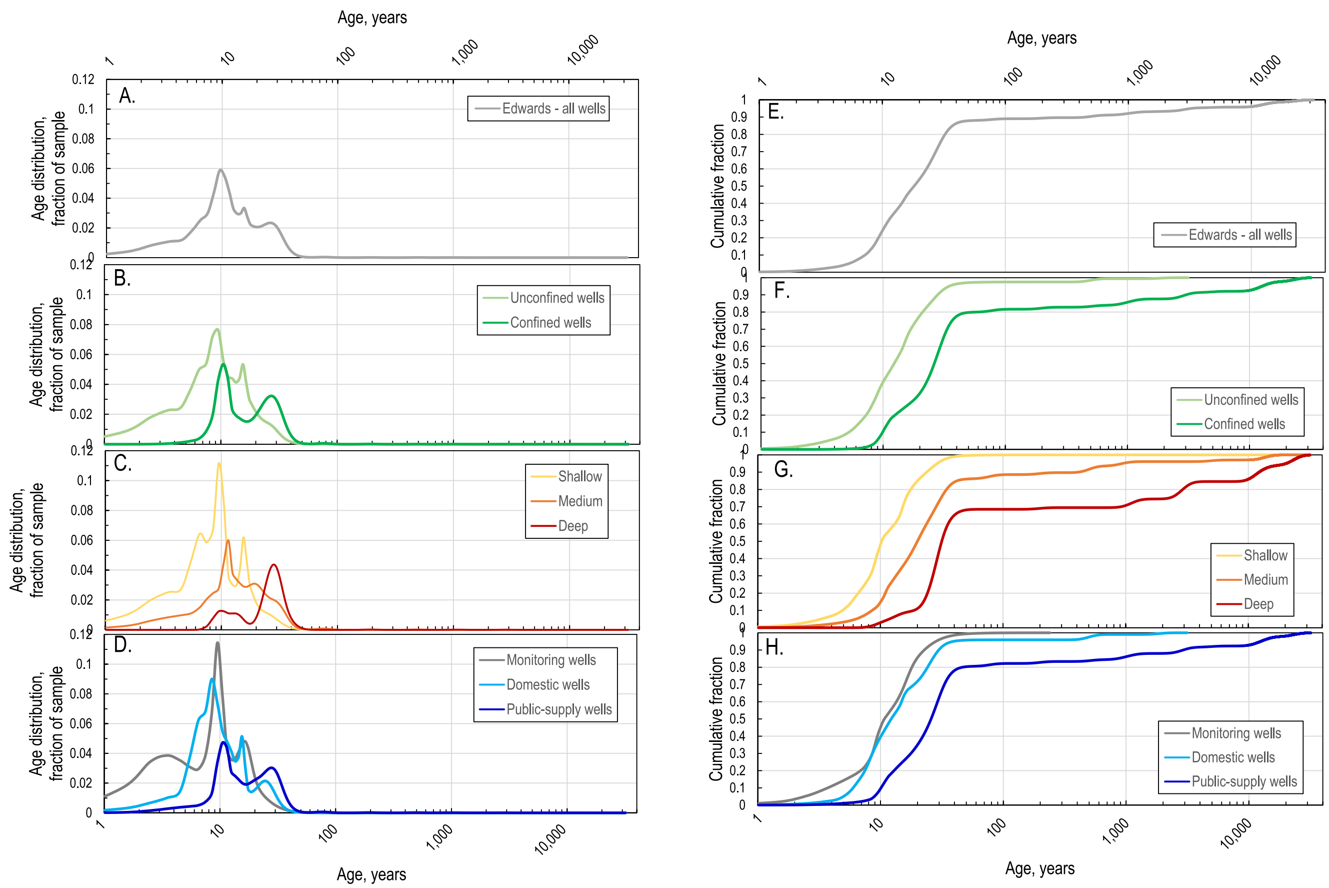

Figure 2. Composite (a–d) and cumulative (e–h) age distributions for Edwards aquifer groundwater. Groupings are: all samples; confined or unconfined zone; well depth—shallow (<92 m), medium (92–305 m), deep (>305 m); well type. Composite age distributions are the average of individual age distributions (assuming equal weighting of individual samples).

LPMs. For BMMs, LPMs estimate ages for a *Modern* (young) fraction and older component, as well as the proportion of the young fraction.

4. Results and Discussion

4.1. Groundwater Age Distributions as Indicators of Vulnerability

Modeled age-tracer results quantify several metrics—the age distribution, mean age, and *Modern* fraction—that collectively quantify an aquifer's vulnerability to contamination. *Modern* groundwater is subject to rapid changes in water quality from anthropogenic contaminants and similarly can rapidly return to background concentrations if contaminant sources are eliminated. In contrast, *PreModern* groundwater is more likely subject to geogenic contamination. In actual fact, any sample is not a single age, but a mixture—composed of water recharging at different times and places (Jurgens et al., 2012). These complexities are especially important for karst because of the contrasting nature of conduit and matrix porosity, each likely representing water of different ages (Long & Putnam, 2006; Plummer & Busenberg, 2005). The mean age is useful for understanding vulnerability and for evaluating spatial patterns (Figure 1); the full age distribution provides a more complete representation of mixing, age, and associated vulnerabilities (Figure 2; also see Figure S2 in Supporting Information S1).

Edwards aquifer groundwater mean ages varied from 4 to 16,900 years (Figure 1). Consistent with preliminary ^{3}H characterizations (Lindsey et al., 2019), samples were predominantly *Modern* (78%), with a lesser amount of *Mixed* (22%), and no *PreModern* groundwater. The median age was 20 years ($n = 60$). The fraction of *Modern* groundwater in *Mixed* samples ranged from 0.11 to 0.89. Thus, even the oldest groundwater contained a substantive fraction of recent recharge. The oldest *PreModern* fraction in *Mixed* samples was 23,500 years.

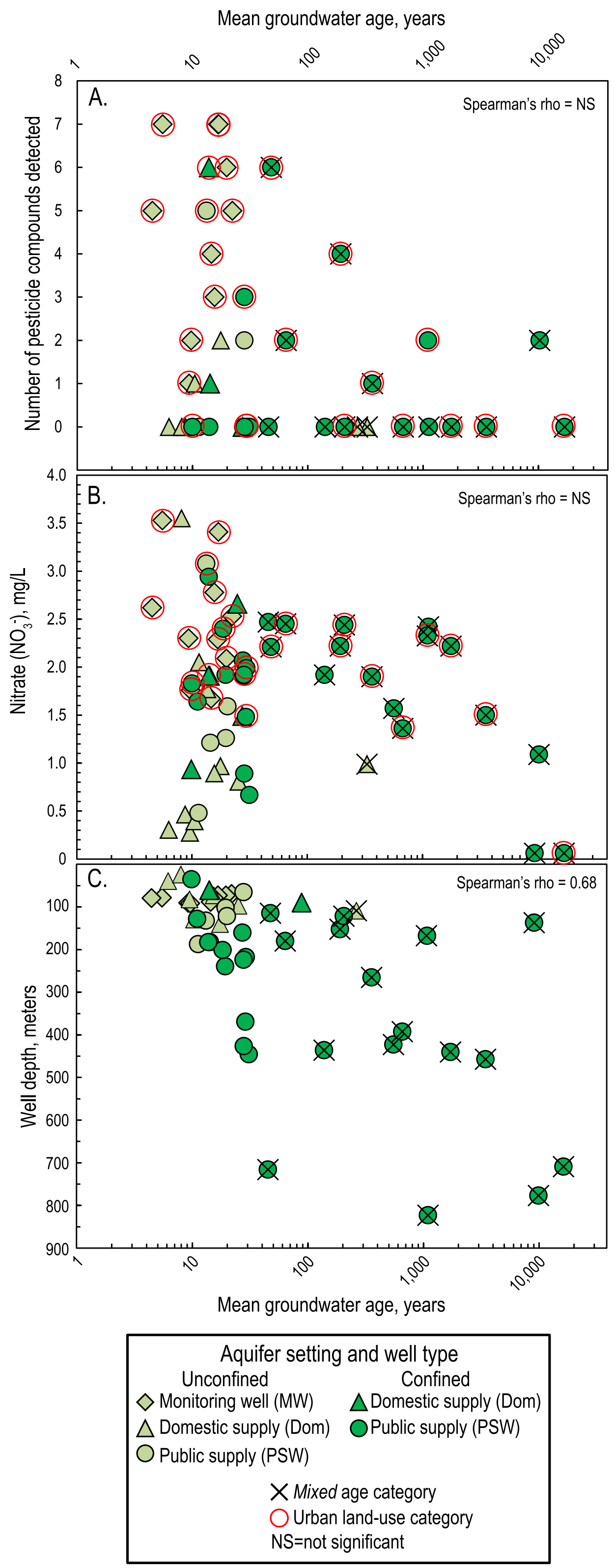

Figure 3. Relations between mean groundwater age and anthropogenic contaminants: (a) number of detected pesticide compounds, (b) nitrate concentration, and (c) well depth. Samples are further distinguished by well type, aquifer setting, *Mixed* age, and wells characterized by urban land use.

The dominance of *Modern* groundwater is typical of carbonate aquifers, which often display a wide range of ages, but tend toward high proportions of *Modern* groundwater (Jurgens et al., 2022).

Edwards aquifer vulnerability can be evaluated regionally by aggregating age distributions for individual samples into composite distributions for different depth categories, confinement, and well type (Figure 2). The age distribution (individually or aggregated), represents the range of ages as the fractional contribution for every year of recharge. Generally, a narrow distribution reflects little dispersion or mixing, suggesting a rapid response to contaminant loading in recharge. A broader and shorter distribution is consistent with more dispersion and mixing, resulting in a larger age range, suggesting a slower response to changes in contaminant loading. A bimodal or multi-modal distribution indicates mixing of groundwater of disparate ages. A bimodal distinction between quick (conduit) and slow (diffuse) flow is characteristic of karst aquifers (Jurgens et al., 2022; White, 1988). These mixtures can arise in wells that draw flow through both conduits and diffuse flow paths. As previously demonstrated for the Edwards aquifer (e.g., Mahler & Massei, 2007), conduit and diffuse flow are typically composed of recent and older recharge, respectively.

Composited age distributions are relatively wide, encompassing a range of ages that tend toward a bimodal distribution (Figure 2). Considering all results, the largest age fraction is centered around 10 years, with a secondary grouping around 30 years (Figure 2a). The cumulative age distribution represents the fraction younger/older than a given age and provides a complimentary visualization tool with additional insight into aquifer vulnerability (Figure 2e) and for comparisons among selected groups of wells (Figures 2f–2h). The cumulative fraction for all results (Figure 2e) indicates that only about 20% of the groundwater is <10 years of age, though the trendline rises steeply between 10 and 40 years, with about 85% of the groundwater younger than 40 years.

In the Edwards aquifer, young, *Modern* groundwater is a necessary but insufficient condition to fully explain contaminant occurrence. We examine common anthropogenic contaminants of concern for groundwater supply: (a) organic contaminants, expressed by the number of detected pesticide compounds, and (b) nutrients, expressed by the concentration of nitrogen (N), specifically as nitrate (NO_3^-N; hereafter NO_3^-). Underscoring concern for these contaminants in the Edwards aquifer, at least one pesticide compound occurred at a concentration exceeding detection levels in 60% of samples and NO_3^- exceeded the estimated groundwater national background concentration (1 mg/L) (Dubrovsky et al., 2010) in >80% of samples. Although both tend to be greater in *Modern* groundwater (Figure 3), the relations are not statistically significant for mean age or the *Modern* fraction (NO_3^- inversely correlates with the *PreModern* fraction) (Table S1 in Supporting Information S1). These results indicate that whereas age is indicative of the intrinsic vulnerability of groundwater to contaminants, additional factors, such as land use or proximity to contaminant sources, also control impacts on groundwater. Such controls are evidenced for the Edwards aquifer, where both the number of detected pesticide compounds and NO_3^- concentrations correlate with the fraction of urban land use (Spearman's rho = 0.60 and 0.41 respectively). Wells with greater detected pesticide compounds and NO_3^- concentrations are predominantly characterized as urban (Figures 3a and 3b).

A lack of *PreModern* groundwater indicates that geogenic contamination is unlikely (Jurgens et al., 2022) and no trace-metal concentrations approached human-health benchmarks (some correlated with age, Table S1 in Supporting

10.1029/2023GL102853

Information S1). Geogenic contaminants often occur with changes in pH and redox (e.g., Degnan et al., 2020). In karst, pH tends to be buffered by the lithology (median groundwater pH was 7.0). Samples were mostly (98%) oxic (dissolved oxygen >0.5 mg/L), so redox effects are unlikely. Because the oldest groundwater occurs near the freshwater/saline-water interface (Figure 1), higher concentrations of some constituents might also occur due to mixing and reaction downdip (Musgrove et al., 2019; Oetting et al., 1996).

4.2. Influence of Regional Hydrology and Well Characteristics

Groundwater age in carbonate aquifers varies systematically as a function of climate and degree of confinement (Jurgens et al., 2022). Aquifer hydrology and well characteristics across the Edwards aquifer influence age metrics and geochemistry. Groundwater age demonstrates consistent regional variability—mean ages generally increase downdip, where the aquifer is confined and deeper in the subsurface due to faulting, and flow paths are typically longer (Figure 1). The oldest ages (>1,000 years; $n = 7$) are primarily downdip near the freshwater/saline-water transition. The median age for the unconfined zone ($n = 28$) was 15 years, whereas the confined zone was 39 years (and significantly different based on a Mann-Whitney U test comparison).

Groundwater age varied consistently with well characteristics. Age increased with well depth (Figure 3c) (Table S1 in Supporting Information S1). Older ages associated with groundwater from deeper wells is an expected relation in porous-media aquifers, where recharge cycles push earlier recharge to deeper depths. Heterogeneous and preferential flow in karst should complicate this relation, with recharge and age patterns reflecting fracture and conduit flow paths rather than traditional age-depth relations. Whereas individual anomalies might be indicative of preferential flow paths or geologic complexities associated with faulting, age and well depth were regionally correlated. Age also varied systematically with well type (Figure 3), which likely partially reflects the sampled well networks, but also their relation with aquifer confinement and depth. Sampled MWs comprise a network of relatively shallow water-table wells in the unconfined/recharge zone. The median age of groundwater from MWs and domestic wells (also primarily unconfined) were similar (15 and 14 years, respectively), but maximum ages reached 22 years for MWs and 9,380 years for domestic wells. PSWs, >80% of which are in the confined aquifer, produce older groundwater, with a median age of 31 years. The oldest groundwater (>1,000 years) is mostly from confined PSWs, which in the Edwards aquifer are typically constructed with large open intervals allowing for mixing of waters from a range of depths and ages in the wellbore (although previous studies indicate that the aquifer is vertically well mixed (Musgrove et al., 2014)); thus, PSW samples are likely to yield relatively old ages, reflecting longer flow paths.

Age distributions for selected well groups—by aquifer confinement, well depth, and well type—further illustrate the influence of regional hydrology and well characteristics (Figures 2b–2d and 2f–2g). As with the regional aquifer (Figures 2a and 2e), age distributions for well groups are characterized by a dominant ∼10-year-age fraction (in the unconfined aquifer, shallow wells, MWs and domestic wells) and a shift toward a second, older ∼30-year-age fraction. The relative importance of the older fraction is most apparent in the confined aquifer, deep wells, and PSWs (Figures 2b–2d); it is dominant in the deep wells (Figure 2c). Nonetheless, even deep, confined PSW groundwater has a distinct ∼10-year age fraction, reinforcing the vulnerability of the regional aquifer to contaminants in recent recharge even for the oldest groundwater. Cumulative age distributions further illustrate this vulnerability (Figures 2e–2h). Well groups (Figures 2f–2h) show similar cumulative distribution patterns as the regional aquifer (Figure 2e), with a rapid rise in the trendline beyond a few years of age. The onset of the rise, however, shifts to the right (older), and the fraction accounted for within a few decades of age decreases for confined and deeper wells and PSWs. Nonetheless, even in the deep wells, most (~65%) of the groundwater is accounted for by ages <40 years.

In karst aquifers, heterogenous flow through conduits and diffuse matrices produce a large range of flow velocities and travel distances that results in complex hydrology over a variety of spatial scales. Whereas regional patterns are useful for understanding holistic aquifer vulnerability and processes, anomalies are also instructive. The vulnerability of individual wells to contamination might be affected by specific or preferential flow paths or localized sources. For example, a domestic well in Medina County with a mean groundwater age of 269 years might be thought largely buffered from anthropogenic effects yet the NO_3^- concentration was 11.5 mg/L (the highest measured), far exceeding the median concentration (1.9 mg/L) and indicating a local contaminant source is likely. This well also exemplifies the vulnerability associated with *Mixed* groundwater; with a modeled young fraction of 8 years comprising 47% of the sample, the mean age alone belies the potential vulnerability to contamination in recent recharge.

10.1029/2023GL102853

4.3. Groundwater Age and Geochemical Tracers of Water-Rock Interaction

We explore the relation of modeled age with independent water-rock interaction tracers that provide insight into processes along aquifer flow paths and can be indicative of groundwater residence time; this is especially likely in karst given the host-rock mineralogy and solubility. Previous studies in carbonate aquifers have described tracers of progressive mineral-solution reactions and groundwater evolution that vary systematically with increased residence time over multiple time scales (e.g., by processes of mineral dissolution, calcite recrystallization, incongruent dolomite dissolution, and prior precipitation of calcite along flow paths). A comparison of these independent tracers, though largely qualitative in nature with respect to residence time, with mean ages, yields relations that reflect both aquifer processes and vulnerability (Figure 4).

Carbon constituents (i.e., dissolved organic carbon [DOC] and carbon isotopes [$\delta^{13}C$]) vary systematically with age; mean age correlates with $\delta^{13}C$ values and inversely with DOC (Spearman's rho = 0.69 and −0.66, respectively) (Figures 4a and 4b). The highest DOC concentrations were in *Modern*, unconfined groundwater, reflecting organic carbon input with recharge (Bakalowicz, 2003). Decreases in DOC along aquifer flow paths by ecological metabolism is a recognized process (e.g., Baker et al., 2000), although the kinetics of DOC attenuation are relatively rapid (Chapelle et al., 2016). These processes are reflected in the Edwards aquifer, where the DOC distribution is largely bimodal. In older groundwater, DOC concentrations are low (at or near detection), indicating that DOC provides insight into recent recharge and active flow paths in the youngest part of the aquifer (e.g., Shen et al., 2015), but is less telling of vulnerability across the large range of ages observed in the Edwards aquifer. In aquifers dominated by young groundwater, DOC would likely provide a useful indicator of vulnerability associated with recent recharge. In contrast, $\delta^{13}C$ values vary more systematically over the full age range; more enriched values trend toward those of the Edwards marine limestone (median of 0.6‰; (Deike, 1991)) and reflect progressive water-rock interaction and carbonate dissolution (Florea, 2013; Katz & Bullen, 1996).

Mg/Ca and Sr/Ca ratios in carbonate aquifers generally increase with longer residence time (e.g., Musgrove & Banner, 2004; Plummer, 1977) and, along with dolomite saturation indices (SIs), correlate with mean age (Spearman's R = 0.29, 0.56, and 0.26, respectively) (Figures 4c–4e). It is likely that relatively invariant Mg/Ca values and dolomite SIs for younger groundwater (around ages <25 years) contribute to their weaker correlation. These tracers are more strongly correlated with the *PreModern* fraction of *Mixed* samples (Spearman's R = 0.69, 0.71, and 0.64, respectively) (Table S1 in Supporting Information S1), indicating their utility over a larger age range in which water-rock interaction processes have progressed along longer flow paths.

Sr isotopes ($^{87}Sr/^{86}Sr$) are tracers of geochemical evolution, weathering, and mixing (Banner, 2004; Dogramaci & Herczeg, 2002; Shand et al., 2009) and trend toward aquifer rock values with increased water-rock interaction (Banner et al., 1994). Edwards aquifer $^{87}Sr/^{86}Sr$ values are significantly different between the unconfined and confined zone but do not correlate with age (Figure 4f), although they correlate (inversely) with Mg/Ca and Sr/Ca ratios, dolomite SIs, and well depth (Spearman's R = −0.73, −0.79, −0.65, and −0.47, respectively). Like DOC, $^{87}Sr/^{86}Sr$ values are somewhat bimodal. Relatively young (i.e., <25 years) unconfined groundwater has a large range, likely reflecting differences in recharge sources, mixing, or conduit and diffuse flow paths. Conversely, older groundwater lies within a narrower range (around 0.7078 and 0.7079) similar to the Cretaceous-age aquifer rocks (Kopenick et al., 1985). These lower $^{87}Sr/^{86}Sr$ values reflect the dominance of progressive chemical interaction of groundwater with the aquifer rocks, whose influence on regional groundwater chemistry is well documented (Musgrove & Banner, 2004; Oetting et al., 1996; Wong et al., 2012).

The hydrologic variability that controls groundwater age is consistently expressed among the various tracers. Along with mean age, all of these tracers are significantly different (based on Mann-Whitney U comparisons) between the aquifer's unconfined and confined zones, and between shallow MWs and deeper PSWs. Such tracers, ideally in combination, can provide insight into aquifer vulnerability as well as an improved understanding of karst processes. Variable tracers are likely better suited to assess different age ranges (e.g., DOC for more recent recharge; Mg/Ca, Sr/Ca, dolomite SIs for older *PreModern* water) reflecting controlling geochemical processes and the hydrologic setting of different karst aquifers.

5. Conclusions

Groundwater age-tracer distributions provide insight into the vulnerability of groundwater to land-surface contamination. Modeled ages increased downdip with well depth regionally in the hydrologically complex,

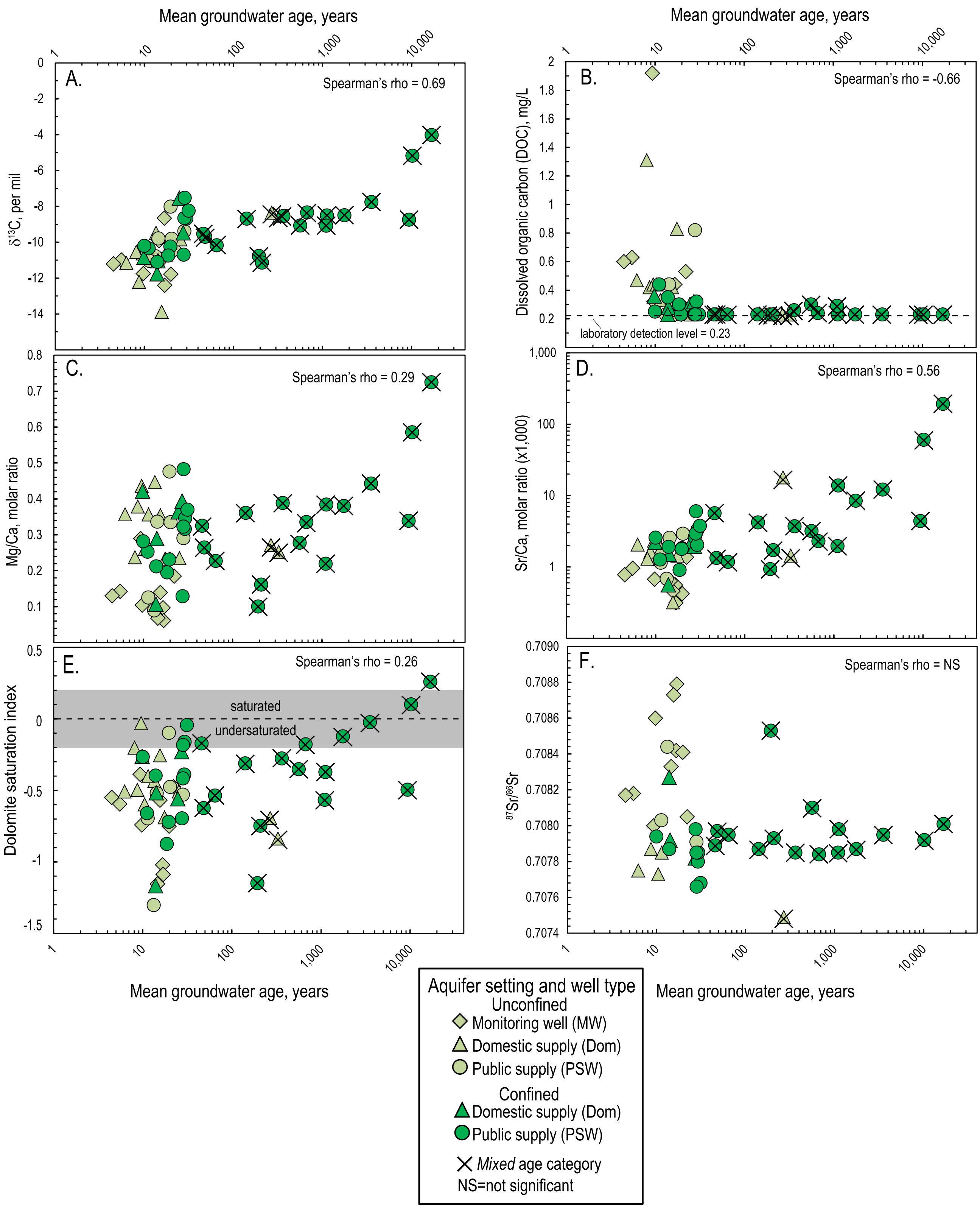

Figure 4. Relations between mean groundwater age and independent geochemical tracers. Samples are further distinguished by well type and aquifer setting.

karstic, Edwards aquifer, in a similar pattern to that expected in porous-media aquifers—a relation that should be considered when assessing vulnerability in other karst aquifers. While *Modern* groundwater is most vulnerable to anthropogenic contamination, older water with a mean age of hundreds or thousands of years remains vulnerable due to mixing with *Modern* recharge. These results are consistent with the aquifer's hydrogeology, recharge dynamics, and regional flow paths, indicating that the unconfined and shallow part of the aquifer contains the youngest, most vulnerable groundwater, while illustrating that the entire aquifer is potentially vulnerable to anthropogenic contamination in recent recharge. We compare groundwater ages with independent tracers of residence time with specific utility in karst aquifers. Although age tracers are requisite for a quantitative assessment of vulnerability, other tracers have potential to yield proxies for groundwater residence time and to provide insight into associated vulnerability in karst aquifers.

Conflict of Interest

The authors declare no conflicts of interest relevant to this study.

Data Availability Statement

All data, calculations, and model output are publicly accessible and archived in the USGS Data Release by Musgrove et al., 2023 (https://doi.org/10.5066/P9CWM574). Analytical measurements and site information are also publicly available online through the USGS National Water Information System (NWIS, https://waterdata.usgs.gov/nwis). Groundwater ages and age distributions were computed using publicly available USGS software programs DGMETA (Jurgens et al., 2020) and TracerLPM (Jurgens et al., 2012), versions of which are available at websites listed in the references.

Acknowledgments
This study was part of the U.S. Geological Survey (USGS) National Water-Quality Assessment Project (https://water.usgs.gov/nawqa/studies/gwtrends/) and was done in collaboration with the San Antonio Water System. Any use of trade, firm, or product names is for descriptive purposes only and does not imply endorsement by the U.S. Government. We thank James R. Degnan (U.S. Geological Survey) and anonymous journal reviews for helpful suggestions that improved this manuscript. We thank landowners and water suppliers for access to wells and USGS colleagues for support in sample collection and data management.

References

Ashworth, J. B., & Hopkins, J. (1995). Aquifers of Texas. Texas water development board report 345. Retrieved from https://www.twdb.texas.gov/publications/reports/numbered_reports/doc/R345/R345Complete.pdf

Bakalowicz, M. (2003). Natural organic carbon in groundwater. *C.R. Geoscience*, *335*(5), 423–424. https://doi.org/10.1016/S1631-0713(03)00085-3

Baker, M. A., Valett, H. M., & Dahm, C. N. (2000). Organic carbon supply and metabolism in a shallow groundwater ecosystem. *Ecology*, *81*(11), 3133–3148. https://doi.org/10.1890/0012-9658(2000)081[3133:OCSAMI]2.0.CO;2

Banner, J. L. (2004). Radiogenic isotopes: Systematics and applications to earth surface processes and chemical stratigraphy. *Earth-Science Reviews*, *65*(3–4), 141–194. https://doi.org/10.1016/S0012-8252(03)00086-2

Banner, J. L., Musgrove, M., & Capo, R. (1994). Tracing ground-water evolution in a limestone aquifer using Sr isotopes: Effects of multiple sources of dissolved ions and mineral-solution reactions. *Geology*, *22*(8), 687–690. https://doi.org/10.1130/0091-7613(1994)022<0687:TGWEIA>2.3.CO;2

Bowles, D. E., & Arsuffi, T. L. (1993). Karst aquatic ecosystems of the Edwards Plateau region of central Texas, USA: A consideration of their importance, threats to their existence, and efforts for their conservation. *Aquatic Conservation: Marine and Freshwater Ecosystems*, *3*(4), 317–329. https://doi.org/10.1002/aqc.3270030406

Chapelle, F. H., Shen, Y., Strom, E. W., & Benner, R. (2016). The removal kinetics of dissolved organic matter and the optical clarity of groundwater. *Hydrogeology Journal*, *24*(6), 1413–1422. https://doi.org/10.1007/s10040-016-1406-y

Degnan, J. R., Lindsey, B. D., Levitt, J. P., & Szabo, Z. (2020). The relation of geogenic contaminants to groundwater age, aquifer hydrologic position, water type, and redox conditions in Atlantic and Gulf Coastal Plain aquifers, eastern and south-central USA. *Science of the Total Environment*, *723*, 137835. https://doi.org/10.1016/j.scitotenv.2020.137835

Deike, R. G. (1991). Comparative petrology of cores from two test wells in the eastern part of the Edwards aquifer, South-Central Texas. *U.S. geological survey water-resources investigations report 87-4266*. https://doi.org/10.3133/wri874266

Dogramaci, S. S., & Herczeg, A. L. (2002). Strontium and carbon isotope constraints on carbonate-solution interactions and inter-aquifer mixing in groundwaters of the semi-arid Murray Basin, Australia. *Journal of Hydrology*, *262*(1–4), 50–67. https://doi.org/10.1016/S0022-1694(02)00021-5

Dubrovsky, N. M., Burow, K. R., Clark, G. M., Gronberg, J. M., Hamilton, P. A., Hitt, K. J., et al. (2010). The quality of our Nation's waters—Nutrients in the Nation's streams and groundwater, 1992–2004. *US Geological Survey Circular*, *1350*. https://doi.org/10.3133/cir1350

Falcone, J. A. (2015). U.S. conterminous wall-to-wall anthropogenic land use trends (NWALT), 1974-2012. *U.S. Geological Survey Data Series*, *948*. https://doi.org/10.3133/ds948

Ferguson, G., Cuthbert, M. O., Befus, K., Gleeson, T., & McIntosh, J. C. (2020). Rethinking groundwater age. *Nature Geoscience*, *13*(9), 592–594. https://doi.org/10.1038/s41561-020-0629-7

Florea, L. J. (2013). Isotopes of carbon in a karst aquifer of the Cumberland Plateau of Kentucky, USA. *Acta Carsologica*, *42*(2–3), 277–289. https://doi.org/10.3986/ac.v42i2-3.668

Ford, D., & Williams, P. (2007). *Karst hydrogeology and geomorphology*. John Wiley and Sons Ltd.

Griffiths, J. F., & Strauss, R. F. (1985). The variety of Texas weather. *Weatherwise*, *38*(3), 137–141. https://doi.org/10.1080/00431672.1985.9933301

Hartmann, A., Jasechko, S., Gleeson, T., Wagner, T., Andreo, B., Barberá, J. A., et al. (2021). Risk of groundwater contamination widely underestimated because of fast flow into aquifers. *Proceedings of the National Academy of Sciences of the United States of America*, *118*(20), e2024492118. https://doi.org/10.1073/pnas.2024492118

Hess, J. W., & White, W. B. (1988). Storm response of the karstic carbonate aquifer of south central Kentucky. *Journal of Hydrology*, *99*(3–4), 235–252. https://doi.org/10.1016/0022-1694(88)90051-0

Humphreys, W. F. (2011). Management of groundwater species in karst environments. In P. E. vanBeynen (Ed.), *Karst management* (pp. 283–318). Springer, Berlin/Heidelberg.

Jasechko, S., Perrone, D., Befus, K. M., Cardenas, M. B., Ferguson, G., Gleeson, T., et al. (2017). Global aquifers dominated by fossil groundwaters but wells vulnerable to modern contamination. *Nature Geoscience*, *10*(6), 5425–5429. https://doi.org/10.1038/ngeo2943

Jurgens, B. C., Böhlke, J. K., & Eberts, S. M. (2012). TracerLPM (Version 1): An Excel® workbook for interpreting groundwater age distributions from environmental tracer data. *U.S. Geological survey techniques and methods report 4-F3*. https://doi.org/10.3133/tm4F3

Jurgens, B. C., Böhlke, J. K., Haase, K. H., Busenberg, E., Hunt, A. G., & Hansen, J. A. (2020). DGMETA (Version 1): Dissolved gas modeling and environmental tracer analysis computer program. *U.S. Geological Survey Techniques and Methods Report 4-F5*. https://doi.org/10.3133/tm4F5

Jurgens, B. C., Faulkner, K., McMahon, P. B., Hunt, A. G., Casile, G., Young, M. B., & Belitz, K. (2022). Over a third of groundwater in USA public-supply aquifers is Anthropocene-age and susceptible to surface contamination. *Nature Communications Earth & Environment*, *3*(1), 153. https://doi.org/10.1038/s43247-022-00473-y

Katz, B. G., & Bullen, T. D. (1996). The combined use of $^{87}Sr/^{86}Sr$ and carbon and water isotopes to study the hydrochemical interaction between groundwater and lakewater in mantled karst. *Geochimica et Cosmochimica Acta*, *60*(24), 5075–5087. https://doi.org/10.1016/S0016-7037(96)00296-7

Kingsbury, J. A., Bexfield, L. M., Arnold, T., Musgrove, M., Erickson, M. L., Degnan, J. R., et al. (2021). Groundwater-quality and select quality-control data from the national water-quality assessment project, January 2017 through December 2019. *U.S. Geological Survey Data Series*, *1136*. https://doi.org/10.3133/ds1136

Kopenick, R. B., Burke, W. H., Denison, R. E., Hetherington, E. A., Nelson, H. F., Otto, J. B., & Waite, L. E. (1985). Construction of the seawater 87Sr/86Sr curve for the Cenozoic and Cretaceous: Supporting data. *Chemical Geology*, *58*, 55–81. https://doi.org/10.1016/0168-9622(85)90027-2

Lindgren, R. J., Dutton, A. R., Hovorka, S. D., Worthington, S. R. H., & Painter, S. (2004). Conceptualization and simulation of the Edwards aquifer, San Antonio region, Texas. *U.S. Geological Survey Scientific Investigations Report 2004–5277*. https://doi.org/10.3133/sir20045277

Lindsey, B. D., Jurgens, B. C., & Belitz, K. (2019). Tritium as an indicator of modern, mixed, and premodern groundwater age. *U.S. Geological Survey Scientific Investigations Report 2019–5090*. https://doi.org/10.3133/sir20195090

Long, A. J., & Putnam, L. D. (2006). Translating CFC-based piston ages into probability density functions of ground-water age in karst. *Journal of Hydrology*, *330*(3–4), 735–747. https://doi.org/10.1016/j.jhydrol.2006.05.004

Maclay, R. W., & Small, T. A. (1983). Hydrostratigraphic subdivisions and fault barriers of the Edwards aquifer, south-central Texas, U.S.A. *Journal of Hydrology*, *61*(1–3), 127–146. https://doi.org/10.1016/0022-1694(83)90239-1

Mahler, B. J., & Massei, N. (2007). Anthropogenic contaminants as tracers in an urbanizing karst aquifer. *Journal of Contaminant Hydrology*, *91*(1–2), 81–106. https://doi.org/10.1016/j.jconhyd.2006.08.010

Musgrove, M., & Banner, J. L. (2004). Controls on the spatial and temporal variability of vadose dripwater geochemistry—Edwards aquifer, central Texas. *Geochimica et Cosmochimica Acta*, *68*(5), 1007–1020. https://doi.org/10.1016/j.gca.2003.08.014

Musgrove, M., Jurgens, B. C., & Opsahl, S. P. (2023). *Data for karst groundwater vulnerability determined by tracers of residence time and age*. U.S. Geological Survey Data Release. https://doi.org/10.5066/P9CWM574

Musgrove, M., Katz, G. G., Fahlquist, L. S., Crandall, C. A., & Lindgren, R. J. (2014). Factors affecting public-supply well vulnerability in two karst aquifers. *Ground Water*, *52*(S1), 63–75. https://doi.org/10.1111/gwat.12201

Musgrove, M., Opsahl, S. P., Mahler, B. J., Herrington, C., Sample, T. L., & Banta, J. R. (2016). Source, variability, and transformation of nitrate in a regional karst aquifer: Edwards aquifer, central Texas. *Science of the Total Environment*, *568*, 457–469. https://doi.org/10.1016/j.scitotenv.2016.05.201

Musgrove, M., Solder, J. E., Opsahl, S. P., & Wilson, J. T. (2019). Timescales of water-quality change in a karst aquifer, south-central Texas. *Journal of Hydrology X*, *4*, 10004. https://doi.org/10.1016/j.hydroa.2019.100041

Oetting, G. C., Banner, J. L., & Sharp, J. M., Jr. (1996). Regional controls on the geochemical evolution of saline groundwaters in the Edwards aquifer, central Texas. *Journal of Hydrology*, *181*(1–4), 251–283. https://doi.org/10.1016/0022-1694(95)02906-0

Plummer, L. N. (1977). Defining reactions and mass transfer in part of the Floridan aquifer. *Water Resources Research*, *13*(5), 801–812. https://doi.org/10.1029/WR013i005p00801

Plummer, L. N., & Busenberg, E. (2005). Chlorofluorocarbons. In P. G. Cook & A. Herczeg (Eds.), *Environmental tracers in subsurface hydrology* (pp. 441–478). Boston, MA: Kluwer Academic Publishers. https://doi.org/10.1007/978-1-4615-4557-6

Schultz, A. L. (1994). 1994 review and update of the position of the Edwards aquifer freshwater/saline-water interface from Uvalde to Kyle, Texas. *Edwards Underground Water District Report*, 94-05. Retrieved from https://www.edwardsaquifer.org/science-maps/research-scientific-reports/science-document-library/

Shand, P., Darbyshire, D. P. F., Love, A. J., & Edmunds, W. M. (2009). Sr isotopes in natural waters: Applications to source characterization and water-rock interaction in contrasting landscapes. *Applied Geochemistry*, *24*(4), 574–586. https://doi.org/10.1016/j.apgeochem.2008.12.011

Sharp, J. M., Jr., & Banner, J. L. (1997). The Edwards aquifer: A resource in conflict. *Geological Society of America Today*, *7*, 1–9.

Shen, Y., Chapelle, F. H., Strom, E. W., & Benner, R. (2015). Origins and bioavailability of dissolved organic matter in groundwater. *Biogeochemistry*, *122*(1), 61–78. https://doi.org/10.1007/s10533-014-0029-4

Smith, B. A., Hunt, B. B., & Schindel, G. (2005). Groundwater flow in the Edwards aquifer: Comparison of groundwater modeling and dye trace results. In *Proceedings 10th multidisciplinary conference on sinkholes and the engineering and environmental impacts of karst*. American Society of Civil Engineers, San Antonio, TX. Retrieved from https://bseacd.org/uploads/Smith-et-al_-Sinkhole-Conf-2005.pdf

Solder, J. E., Jurgens, B., Stackelberg, P. E., & Shope, C. L. (2020). Environmental tracer evidence for connection between shallow and bedrock aquifers and high intrinsic susceptibility to contamination of the conterminous U.S. glacial aquifer. *Journal of Hydrology*, *583*, 124505. https://doi.org/10.1016/j.jhydrol.2019.124505

Stevanović, Z. (2019). Karst waters in potable water supply: A global scale overview. *Environmental Earth Sciences*, *78*(23), 662. https://doi.org/10.1007/s12665-019-8670-9

Texas Water Development Board. (2007). GIS data—Major aquifers. Retrieved from https://www.twdb.texas.gov/mapping/gisdata.asp

U.S. Census Bureau. (2022). QuickFacts. Retrieved from https://www.census.gov/quickfacts/fact/table/US/PST045221

U.S. Environmental Protection Agency. (2022). Sole source aquifers for drinking water. Retrieved from https://www.epa.gov/dwssa

White, W. B. (1988). *Geomorphology and hydrology of karst terrains*. New York, NY: Oxford University Press.

Wong, C. I., Mahler, B. J., Musgrove, M., & Banner, J. L. (2012). Changes in sources and storage in a karst aquifer during a transition from drought to wet conditions. *Journal of Hydrology*, *9*, 159–172. https://doi.org/10.1016/j.jhydrol.2012.08.030